COLUMN INTERACTION IN TUFTED SANDWICH STRUCTURES UNDER EDGEWISE LOADING

Jamie W. Hartley*, Gavin Tse, James Kratz, Carwyn Ward and Ivana Partridge

Advanced Composites Centre for Innovation and Science, University of Bristol, Queens Building, University Walk, Bristol BS8 1TR, UK
*Email: jh9799@bristol.ac.uk, Web Page: http://www.bristol.ac.uk/composites

Keywords: 3-Dimensional Reinforcement, Sandwich, Mechanical Testing, Tufting

Abstract
Tufted sandwich panels have been shown to be effective energy absorbing structures when subjected to in-plane compressive loads, such as those exhibited during an automotive vehicle side impact. However, up to now, no focus has been paid to understanding the complex failure mechanisms that take place during this type of loading, in particular what happens to the individual tufts, both during and after failure. In this study, an experimental test procedure was used to observe the behaviour of tufts during edgewise crushing. Overall, the tufted samples showcased a prolonged and more stable failure than the untufted baseline. The test also showed a clear drifting and stacking motion of the tufts, as well as highlighting a number of secondary failure mechanisms that take place, that have not been documented before. Further understanding of how these occur could lead to better performance and controllability of the global failure of such a structure.

1. Introduction

Sandwich assemblies offer very high levels of structural efficiency by delivering increased stiffness and strength for a relatively low increment of weight. A limiting factor of these materials when subjected to in-plane crushing is their poor resistance to inter-ply delamination, and disbonding of the skins, ultimately reducing mechanical performance [1].

Through-Thickness Reinforcement (TTR) can improve these properties, acting as a mechanical joint between the skins and altering the failure mechanisms of the component [2]. Tufting is one such TTR method, which uses a single needle to pass loops of thread through the panel [3], and mechanically connect the two skins together. Unlike more traditional stitching methods it only requires access to one side of the preform, and demonstrates the potential for a reduced degradation of the in-plane properties of the final composite [4]. Previous work has shown the effectiveness of tufted sandwich structures, both for face impact [5] and static and dynamic edgewise loading [6].

One of the notable features of tufting sandwich panels is the relatively large column of resin formed around the tufts (Figure 1). This is due to the brittle nature of the foam core, which fragments and leaves behind a void after needle insertion. As the needle used (~2 mm) is typically much larger than the tufting thread (~0.3 mm), a void is left within the core that fills with resin during infusion of the part.

Excerpt from ISBN 978-3-00-053387-7

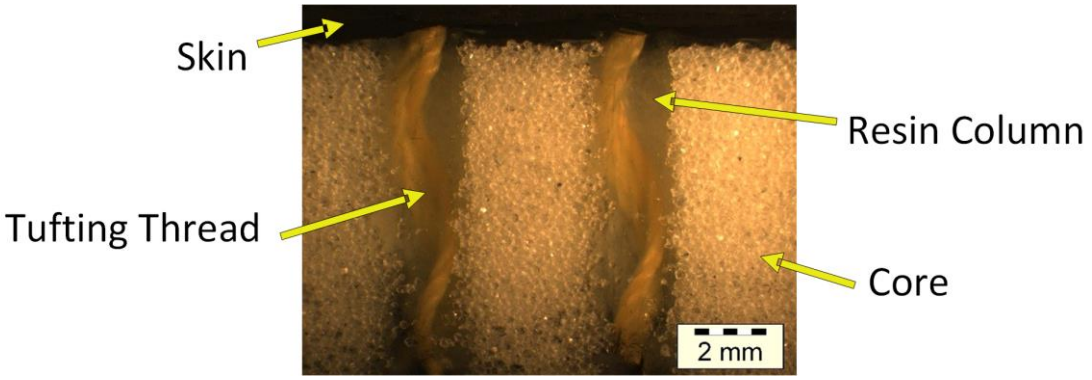

Figure 1. Resin columns formed during tufting.

A recent study investigated the behaviour of design variables on the behaviour of individual tufts [7]. This study considered the effect of the loop length of a tuft as well as the number of threads used. One of the observations made during this investigation was that the tufts and resin columns became detached after failure and a drifting mechanism of the tuft column took place during crushing.

The aim of this research is to investigate this behaviour further, with a particular focus on the potential interactions that could take place if multiple tufts are used, and collisions between tufts are allowed to take place. Mechanical crushing of representative tufted test coupons will be carried out, and digital characterisation techniques used to track the behaviour of the tufts as they fail.

2. Method

2.1. Specimen Manufacture

A tufted sandwich panel was manufactured using the Vacuum-Assisted Resin Transfer Moulding (VARTM) technique. The preform was assembled using a uniweave carbon fibre fabric from SGL Automotive (300 g/m^2), and a Rohacell® 110 IG-F closed-cell foam by Evonik (110 kg/m^3) for the core. The chosen layup was $[0/90/0]_s$, giving a 2 mm thick skin. The preform was heated for 2 hours at 90 ˚C under vacuum pressure to activate the binder in the carbon fabric before tufting using the robotic tufting unit at the UK National Composites Centre. A polystyrene backing sheet was placed below the preform to allow the needle to pass through the preform and form the loops on the backside. A nylon film was placed between the preform and the backing sheet to assist removal of the preform after tufting. The tufts were formed using a Tkt-20 Kevlar thread using a 6 mm x 6 mm tuft spacing. The final tufted preform was then infused at 40 ˚C using EPIKOTE® Resin RIM 935 and EPIKURE® Curing Agent RIM 936 by Momentive. The cure cycle was two hours at 60 ˚C, one hour at 80 ˚C and a one hour post-cure at 90 ˚C.

After cure the test coupons were cut using a diamond saw to the dimensions shown in Figure 2. The length of the test coupon was varied to provide differing numbers of tufts, creating 3 different coupon configurations. A further set of untufted baseline samples were also created for comparison. A small amount of polishing, using a Buehler MetaServ 250 polishing machine, was carried out on one surface of each coupon to reveal the tuft columns at that face, to allow them to be tracked.

Excerpt from ISBN 978-3-00-053387-7

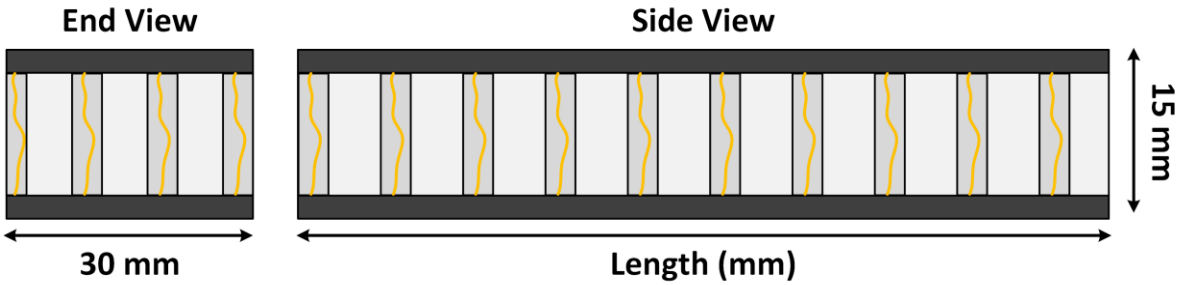

Figure 2. Test coupon dimensions.

Table 1. Test Configuration Summary

Group	*Length*	*Mass*
-	*mm (±0.3)*	*g (±1)*
Baseline	50	13
A	40	12
B	50	16
C	60	19

2.2. Test Procedure

Testing was carried out under quasi-static loading conditions using a Zwick 1466 test machine. Coupons were clamped at the base within an end support fixture, and positioned at the centre of the loading plates, to ensure failure occurred at the free end of the coupon. Coupons were aligned such that the long edge was parallel to the crushing direction, with the polished face exposed for tracking. A displacement control program was used to provide a constant quasi-static crushing rate of 2 mm/min. Testing was terminated after crushing had reached the final tuft before the fixture. A total of 3 coupons were tested per configuration. An Imetrum® video gauge system was used to track the movement of the tuft columns at the edge of the coupon. This camera system was able to track the movement of individual pixels within an image, thus following the movement of the tufts as the coupon was crushed. White paint marks were placed on each tuft to act as clear tracking points. The system also allowed video playback of test, allowing failure mechanisms to be viewed and identified.

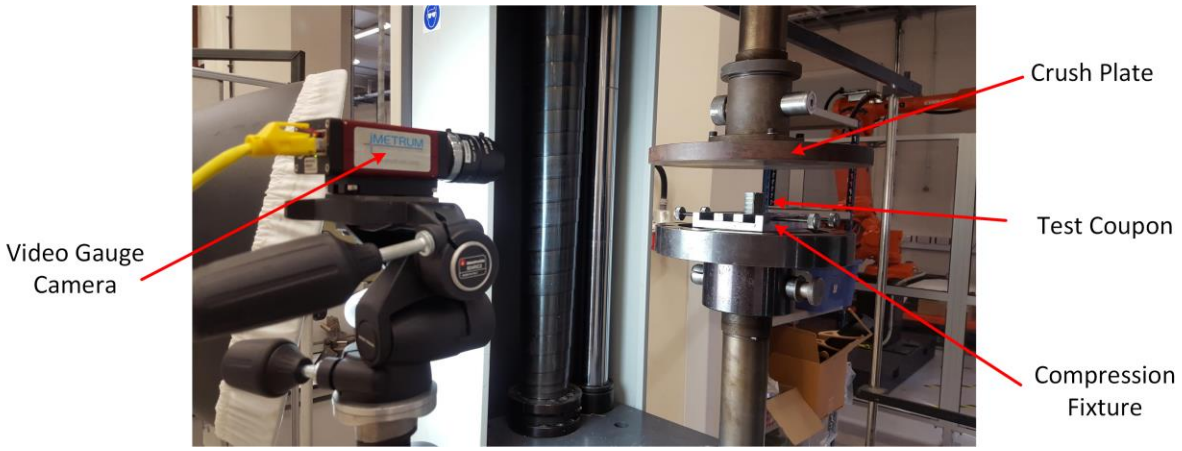

Figure 3. Test setup.

Excerpt from ISBN 978-3-00-053387-7

3. Results and Discussion

Results of the testing showed a clear difference in failure mode between the tufted and untufted coupons. Failure of the untufted baseline coupons exhibited an unstable collapse, due to global buckling of the coupon as well as separation between the skin and core. In contrast, the tufted coupons predominantly showed a more stable, progressive splaying mode. These failure modes are what would typically be expected for sandwich structures during crushing, as discussed in [1]. The contrasting failure modes are shown in Figure 4.

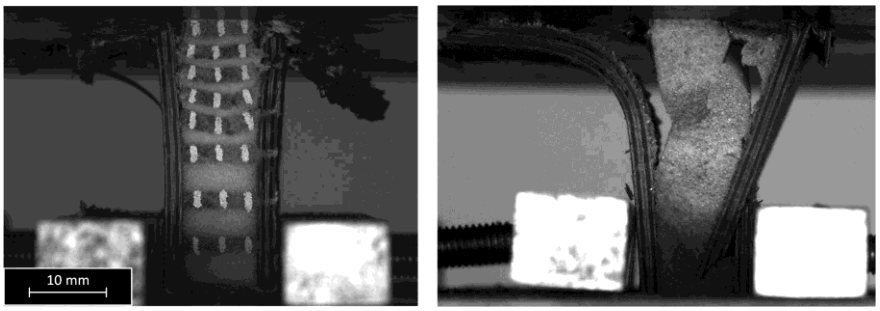

Figure 4. Failure mode comparison, **Left:** Stable crushing in tufted samples. **Right:** Unstable collapse in baseline samples.

Figure 5 represents a typical load-displacement curve for tufted and untufted coupons, highlighting the difference in performance between the two. Both coupon types show a typical loading response for composite structures during crushing, a sharp peak followed by a sustained crushing force, as outlined in [8]. For the untufted coupon, the load peaks at 35kN (region 1), followed by a significant drop to around 5kN as the coupon collapses. This loading is sustained until around 20 mm of displacement where the coupon fails completely and the test is stopped. Whilst the tufted coupon peaks at a similar load value, in contrast the coupon is able to sustain a much greater load, around 50% of the initial peak. The tufted coupon is also able to sustain the load over a longer crushing distance, showing an increase in length of at least 50%, with the potential for more, as testing was terminated at the fixture, before complete failure of the coupon. Region 2 in Figure 5 highlights a significant drop in load of the tufted coupon. At this point, a relatively large crack appeared at the skin-core interface and resulted in a kinking and fracturing of the skin. However after this drop the tufts allow the coupon to recover the load again.

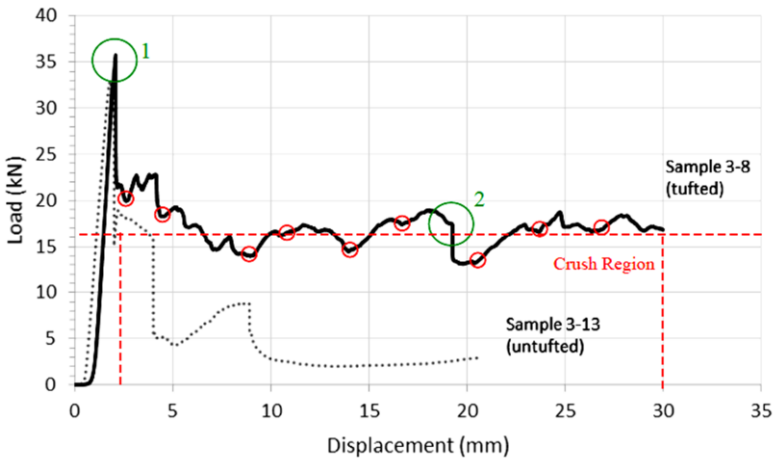

Figure 5. Representative load-displacement plot of a tufted and untufted test coupon.

Excerpt from ISBN 978-3-00-053387-7

3.1 Column Motion

Video tracking during testing showed that in-plane movement of the tufts took place, in the direction of the applied crushing force. As these columns began to drift they would come into contact with each other and began to stack. An overview of this process is shown in Figure 6.

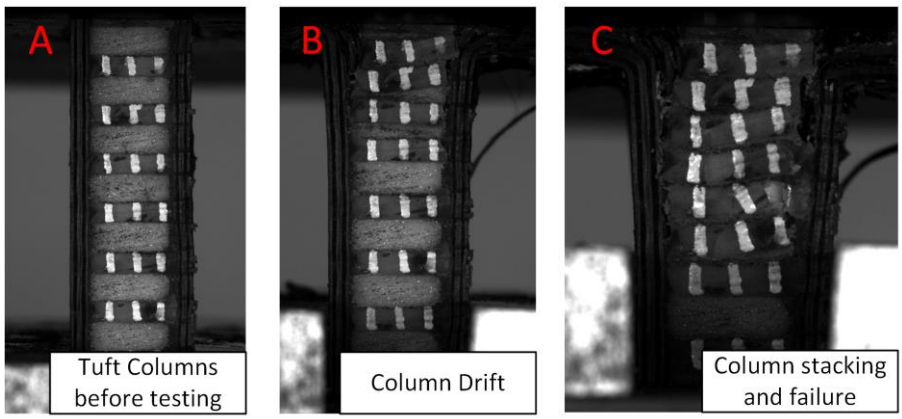

Figure 6. Drift and stacking of tuft columns (white marks used for video tracking).

Tracking of the tufts was carried out both in the direction of crushing and perpendicular to this. Tracking of the in-plane movement (Figure 7) supports the image shown in Figure 6, but also highlights the stability of the process. The tufts appeared to fail at a constant rate with no sudden unstable jumps. On the other hand, the perpendicular displacement showed a change of direction in the movement. This was because one skin would typically fail before the other, which resulted in tuft failure at only one end, pulling the tuft in one direction before it corrected and moved back to its neutral position as the other skin failed (Figure 8).

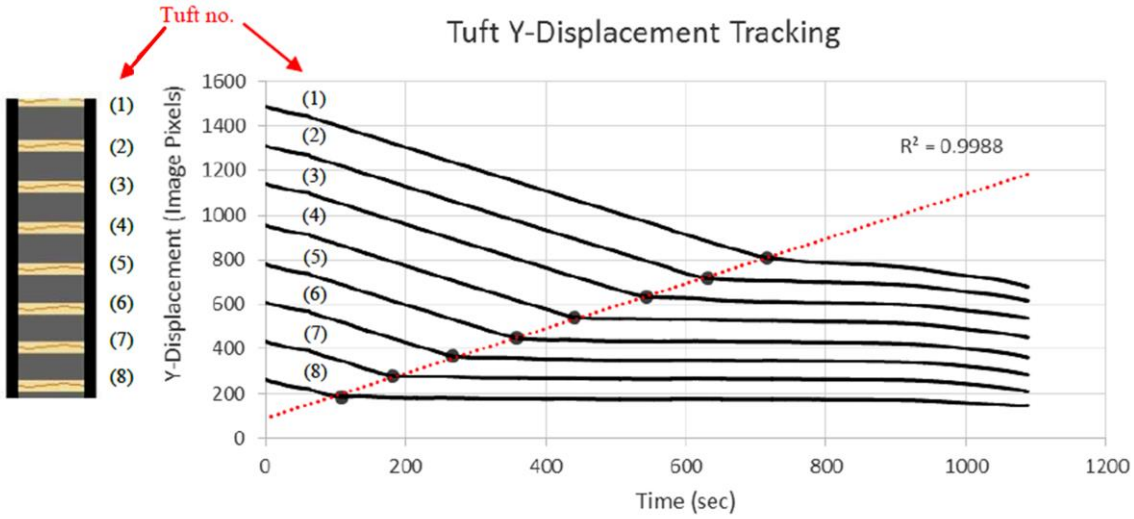

Figure 7. Pixel tracking of tuft movement in crush direction.

Excerpt from ISBN 978-3-00-053387-7

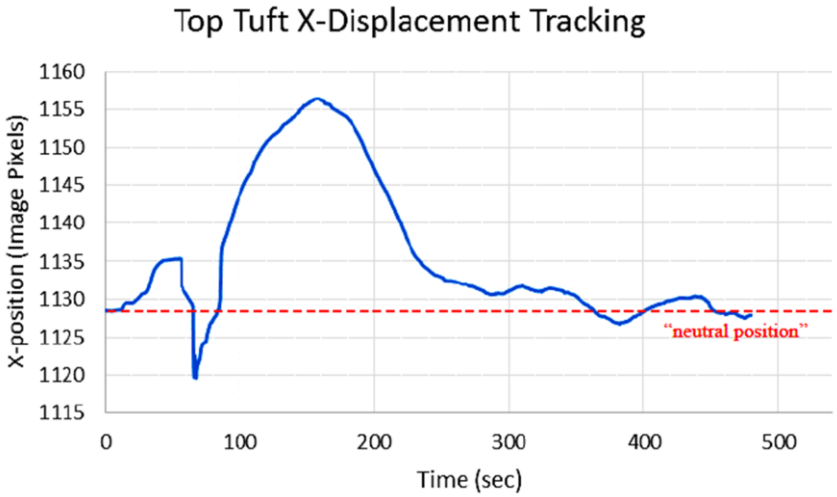

Figure 8. Perpendicular motion and recovery of tufts.

3.1 Local Failure Mechanisms

Further to the column motion, a number of local failure mechanisms around the tufts were also observed at various stages of the crushing process (Figure 9). These were typically highlighted within the load-displacement traces of the individual tests, as shown in Figure 5. The red markers on the tufted curve highlight the point at which the individual tufts are failing. After each point there was a noticeable increase in the load as the column detached and was forced downwards into the core. These additional failure mechanisms will be explored in more detail in the follow section.

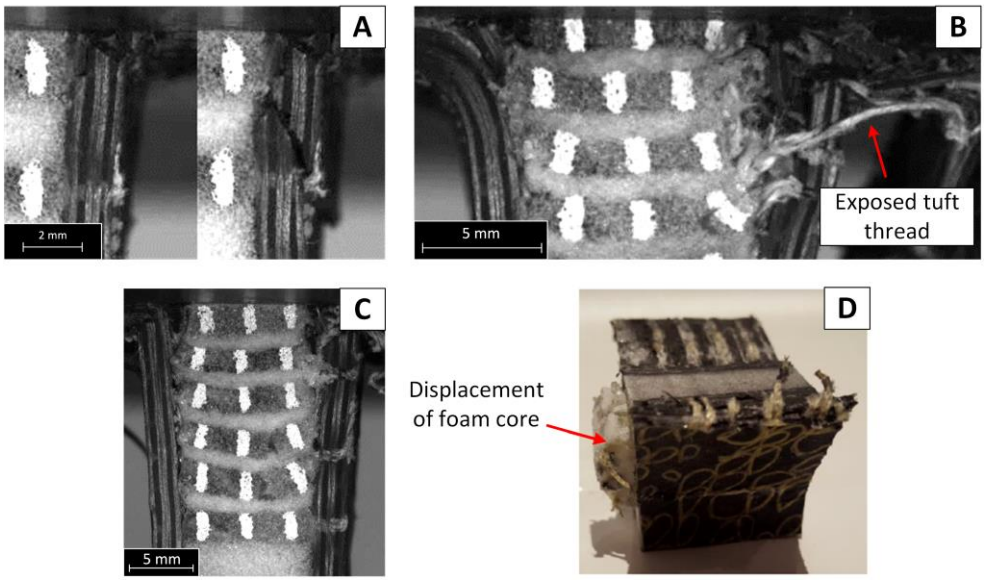

Figure 9. Observed failure mechanisms, **A** Skin fracture, **B** Thread pull-out, **C** Column Bending, **D** Core displacement.

The most common local failure mechanism observed was fracturing of the skins. Initially this took the form of delamination in the outer-most plies, occurring at the top surface of the coupon, where it was in contact with the crush plate. However predominantly skin fracture was observed around tuft sites, as

Excerpt from ISBN 978-3-00-053387-7

shown in Figure 9a, due to the resin rich area formed by the displacement of the fibres around the tuft.

Despite the mostly Mode I opening type failure mode of the coupons, typically failure of the tufts occurred due to shearing at the skin-core interface, however in one isolated case a tufting thread was observed to have pulled out of the resin column (Figure 9b). This is an interesting result as despite tufts providing a reinforcement through-thickness, it is rare for them to fail in tension as a result of the opening of the skins. The reason for this type of failure was not clear, however it could potentially be related to the alignment of the thread within the column when it is loaded, or perhaps a defect in the column that could cause it to fracture around the thread. It was also observed that the location of the tufts relative to the crush site did have some effect on their behaviour. If tufts were positioned close to the upper compression plate, an earlier onset of skin fracture occurred which led to a reduction in the overall compressive strength of the coupon. Also as crushing progressed, the foam closest to the crush front tended to act as a wedge, forcing down onto the tuft columns. Because the columns are fixed at each end, this downward force causes the columns to bend as shown in Figure 9c. In some cases this bending effect caused the columns to crack.

Generally, failure of the core was limited to in-plane crushing as the individual cells of the foam collapsed. In several cases, when the density of the foam reached a point that it could not be compressed further, fracturing took place and large pieces were forced out of the structure as shown in Figure 9d.

3.2 Energy Absorption

Table 2 shows the specific energy absorption values calculated for each coupon. The energy absorption was approximated by integrating the area under the load-displacement curve, and divided by the crushed material mass. As expected by the results in Figure 5, the tufted coupons are able to absorb a significantly larger amount of specific energy, due to the increased load and longer crushing distance. This is despite an increase of the mass due to the tufts.

Table 2. Specific Energy Absorption

Group	Coupon	*Peak Load*	*Energy Absorbed*	*Specific Energy Absorption*
	-	*kN*	*kJ*	*kJ/kg*
A	3-1	25.4	0.212	17.7
	3-2	29.5	0.284	23.7
	3-3	37.9	0.184	15.3
B	3-4	35.18	0.347	23.1
	3-5	23.3	0.243	15.2
	3-6	32.0	0.275	17.2
C	3-7	36.3	0.290	15.3
	3-8	35.7	0.457	24.1
	3-9	21.3	0.354	18.6
Baseline	3-10	33.6	0.571	43.9*
	3-11	32.2	0.108	8.31
	3-12	32.9	0.131	10.1

**Sample 3-10 failed at the test fixture.*

There is significant scatter between coupons, which are partly due to test coupon variations, but more likely to be a result of the large number of failure modes observed across the different tests.

Excerpt from ISBN 978-3-00-053387-7

Understanding how these occur and why will allow them to be exploited in the design of tufted sandwich structures. Aside from this, future work could investigate the behaviour of different material configurations, such as alternative tuft or core materials, or different laminate stacking sequences. Another area of interest could be to explore the effect of off-axis loading, as this would more likely be seen in a real-life application and could drastically change the behaviour of the tufts. Finally the use of a trigger mechanism, and its relationship with the first tuft location could also be considered, to see if the global failure mechanism can be controlled in this way.

4. Conclusions

An experimental testing method has been used to observe and characterise the behaviour of tufts within a sandwich structure under edgewise compression. The test method highlighted a clear drifting mechanism of the tufts, as well as stacking of the columns when the tufts collide. The test further highlighted the stability that tufting provides to sandwich structures under edgewise compression, as previously demonstrated, as well as the significantly improved energy absorption capability of these types of structures. Furthermore, a number of secondary, yet more complex, failure mechanisms that take place around the tufts during crushing were demonstrated, and understanding these could allow even more control of the global performance of these structures.

Acknowledgments

The authors would like to acknowledge funding from the EPSRC Centre for Doctoral Training in Advanced Composites for Innovation and Science (Grant: EP/G036772/1) and the EPSRC Centre for Innovative Manufacturing in Composites (CIMComp) (Grant: EP/IO33513/1).

References

[1] A.G. Mamalis, D.E. Manolakos, M.B. Ioannidis, and D.P. Papapostolou. On the crushing response of composite sandwich panels subjected to edgewise compression: Experimental. *Composite Structures*, 71:246-257, 2005.

[2] K.S. Raju and J.S. Tomblin. Energy Absorption Characteristics of Stitched Composite Sandwich Panels. *Journal of Composite Materials*, 33:712-728, 1999.

[3] G. Dell'Anno, J. W. G. Treiber, and I.K. Partridge. Manufacturing of composite parts reinforced through-thickness by tufting. *Robotics and Computer-Integrated Manufacturing*, 37:262-272, 2016.

[4] G. Dell'Anno, D.D. Cartié, I.K. Partridge, and A. Rezai. Exploring mechanical property balance in tufted carbon fabric/epoxy composites. *Composites Part A: Applied Science and Manufacturing*, 38:2366-2373, 2007.

[5] A. Henao, R. Guzmán de Villoria, J. Cuartero, M. Carrera, J. Picón, and A. Miravete. Enhanced impact energy absorption characteristics of sandwich composites through tufting. *Mechanics of Advanced Materials and Structures*, 22:1016-1023, 2015.

[6] L.G. Blok, J. Kratz, D. Lukaszewicz, S. Hesse, C. Kassapoglou, and C. Ward. Improvement of the in-plane crushing response of CFRP sandwich panels by through-thickness reinforcements. ECCM17 – *Proceedings of the 17th European Conference on Composite Materials ECCM-17, Munich, Germany*, June 26-30 2016.

[7] J. Hartley, J. Kratz, C. Ward, and I Partridge. Observing process parameter effects in tufted sandwich structures. ICMAC 2015 – *Proceedings of the 10th International Conference on Manufacturing of Advanced Composites, Bristol, UK*, June 24-25 2015.

[8] D. H.-J. A. Lukaszewicz. Automotive Composite Structures for Crashworthiness, in *Advanced Composite Materials for Automotive Applications*, John Wiley & Sons Ltd, 2013, pp. 99–127.

Excerpt from ISBN 978-3-00-053387-7